Standard (NRZ 1 × 40 Gb/s, 210 km) and Polarization Multiplex (CS-RZ, 2 × 40 Gb/s, 212 km) Transmissions With PMD Compensation

David Sandel, Frank Wüst, Vitali Mirvoda, and Reinhold Noé

***Abstract*—A single-waveplate polarization scrambler at the transmitter (TX) generates pulse arrival time fluctuations in the presence of polarization-mode dispersion. These were detected with a 680-fs sensitivity in the receiver clock recovery phase-locked loop, thereby enabling a polarization-mode dispersion (PMD) compensated 210-km nonreturn-to-zero transmission. For polarization division multiplex, polarizations were scrambled by an interchannel phase modulation which enabled PMD-compensated CS-RZ 212-km transmission.**

***Index Terms*—Compensation, equalizers, optical fiber communication, optical polarization-mode dispersion, polarization, polarization division multiplex, polarization-mode dispersion.**

I. Introduction

RECENTLY, several polarization-mode dispersion (PMD) detection methods based on polarization scrambling at the transmitter side or degree-of-polarization measurement have been proposed [1]–[5]. Pulse arrival time detection [5] allows to measure PMD in a few μs and without need for dedicated polarimetry. For standard 40-Gb/s transmission we report here on a detection sensitivity that is tripled from its previous value 2 ps, and on a PMD compensation experiment.

If one employs a distributed PMD compensator [6] it is easy to output the PMD-compensated signal with a predefined polarization, as needed for polarization division multiplex (PolDM) transmission [7]–[11]. For polarization control purposes the detrimental interchannel interference may be detected by adding an interchannel phase modulation [8]. Here, this is combined with arrival time detection for a PMD-compensated PolDM transmission experiment.

II. Standard, Single Polarization Transmission

Let the time-variable scrambler output polarization and a principal state-of-polarization (PSP) of a subsequent fiber be denoted by the normalized Stokes vectors $\mathbf{S}_{SC}(t)$ and $\mathbf{S}_{PSP}$, respectively. For a differential group delay (DGD) τ the pulse arrival time is $\Delta\hat{t}(t) = (\tau/2)\mathbf{S}_{PSP}^T\mathbf{S}_{SC}(t)$. A constant root-mean-square (rms) value $\Delta\hat{t}_{rms} = \tau/\sqrt{12}$ is obtained for all $\mathbf{S}_{PSP}$ if the correlation matrix $\langle\mathbf{S}_{SC}(t)\mathbf{S}_{SC}^T(t)\rangle$

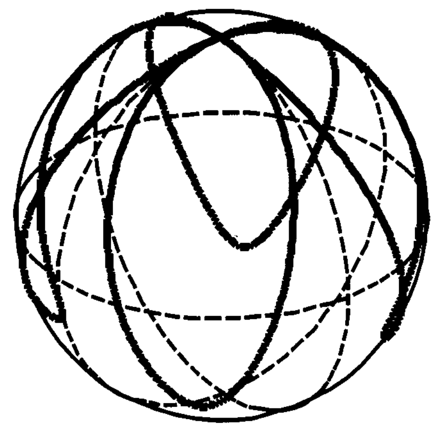

Fig. 1. Calculated scrambler output polarization $\mathbf{S}_{SC}(t)$ trajectory on Poincaré sphere.

equals 1/3 times the unity matrix. A suitable scrambler for circular input polarization was set up, consisting of a single electrooptic waveplate in X-cut, Z-propagation $LiNbO_3$ [12]. In the scrambler, TE-TM phase shift and TE-TM mode conversion alone would be $\varphi_{PS} = 1.12\sin\omega t + 1.12\sin 3\omega t$, $\varphi_{MC} = 1.12\cos\omega t - 1.12\cos 3\omega t$, respectively, but they are applied together to produce a retardation $\varphi = \sqrt{\varphi_{PS}^2 + \varphi_{MC}^2}$ between linearly polarized eigenmodes, one of which has the normalized Stokes vector $[\varphi_{PS}/\varphi\ \varphi_{MC}/\varphi\ 0]^T$ (Fig. 1).

In the transmission setup (Fig. 2) fiber and erbium-doped fiber amplifiers (EDFAs) were initially replaced by a device under test (DUT) and the PMD compensator (PMDC) was left out. A 40-Gb/s nonreturn-to-zero (NRZ) signal was fed into the scrambler. Fundamental scrambling frequency was 104 kHz. The arrival time modulation is tracked by the clock recovery phase-locked loop (PLL) [5]. The voltage-controlled oscillator (VCO) input signal, supplied by a proportional-integral (PI) controller, is roughly the derivative of the signal arrival time. It suffices to integrate the VCO input signal and to measure the standard deviation of this integral. Fig. 3 depicts measured $\Delta\hat{t}_{rms}$ vs. DGD τ of the DUT. Polarization transformers (M) before and behind the DUT were manually adjusted so as to minimize or to maximize $\sigma_{\hat{t}}$. Measured best and worst case averages $\overline{\Delta\hat{t}_{rms}}$ of $\Delta\hat{t}_{rms}$ differed by $\pm 18\%$ at $\tau = 680$ fs and by $\pm 9\%$ at $\tau = 8.6$ ps. This is not critical; it will just cause convergence speed differences of a PMDC depending on the starting point.

For both maximum and minimum sensitivity, the $\pm 1\sigma$ error intervals are also indicated by bars. Measurement sensitivity

Manuscript received February 7, 2002; revised March 28, 2002. This work was supported in part by Siemens ICN and by Deutsche Forschungsgemeinschaft.

The authors are with the Optical Communication and High-Frequency Engineering, Electrical Engineering and Information Technology, Univ. Paderborn, Warburger Str. 100, 33098 Paderborn, Germany (e-mail: noe@upb.de)

Publisher Item Identifier S 1041-1135(02)06074-3.

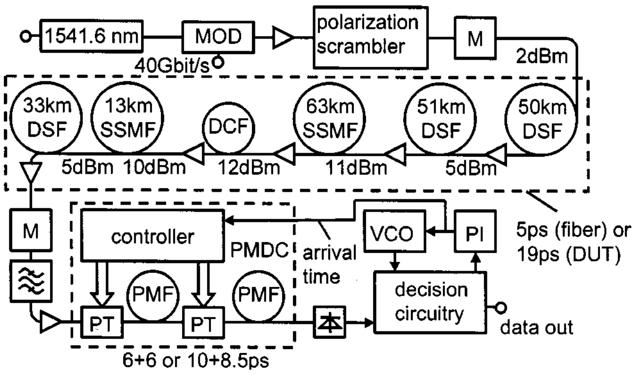

Fig. 2. 40-Gb/s transmission setup using arrival time detection.

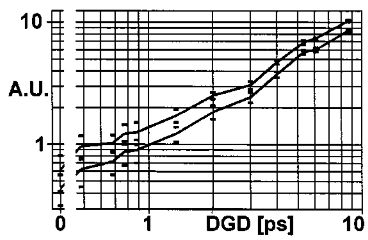

Fig. 3. Measured best (top) and worst-case (bottom) rms arrival time variations Δt_{rms} versus DGD.

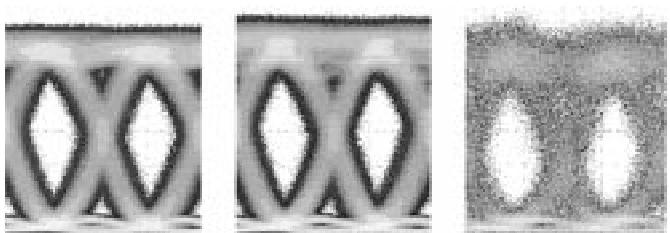

Fig. 4. 40-Gb/s eye diagrams in the presence of endless polarization changes: 10-min persistence back-to-back (left) and with PMDC using 19-ps emulator (middle); 10-s persistence after 210 km with 6 ps + 6 ps PMDC (right).

was defined by nonoverlapping $\pm 1\sigma$ error intervals at a DGD of 680 fs versus a vanishing DGD. The improvement with respect to [5] is due to the scrambler which meets the correlation matrix condition fairly well (unlike the rotating waveplate scrambler used in [5]), improved signal processing and a doubled measurement interval which lasts one scrambling period (9.6 μs).

The receiver (RX) was then completed by the PMDC with two X-cut Z-prop. $LiNbO_3$ polarization controllers (PCs), controlled by a gradient algorithm, and two DGD sections (PMF; 10 ps + 8.5 ps). As a PMD emulator or device under test (DUT) there was as a 19-ps DGD element at the transmitter (TX) side, framed by the two polarization controllers (M) consisting now of 4 motorized endlessly rotating fiber loops each. BER measurement was not possible because a 1:4 demultiplexer (10 Gb/s $\rightarrow 4 \times 2.5$ Gb/s) had failed in the RX. Fig. 4 shows received eye diagrams with a 10-min persistence back-to-back (left), and with DUT and PMDC (middle). The broadening of the ones is due to PDL. With DUT alone the eye diagram was essentially closed. Fig. 5 shows measured recovered clock spectra after prescaling to 10 GHz. With PMDC the sidelines are $\sim$ 30 dB down. Then the DUT was replaced by 210 km

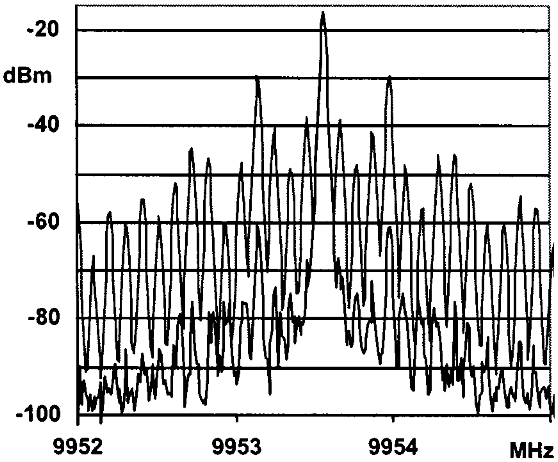

Fig. 5. Prescaled recovered clock spectra in the presence of a 19-ps DGD without (top) and with (bottom) PMD compensation.

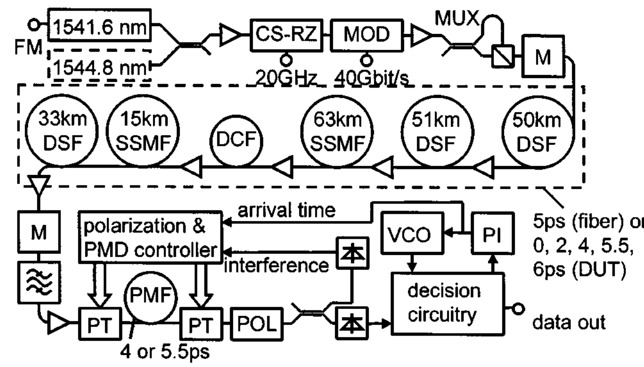

Fig. 6. PolDM transmission with endless polarization control and PMD compensation.

of DSF and SSMF, some DCF, and EDFAs. Total DGD was on the order of 5 ps. The PMDC DGDs were reduced to 6 ps + 6 ps. In order to show any residual arrival time modulation, the eye diagram (Fig. 4 right) was again triggered from the TX, but due to thermal propagation delay drift a shorter persistence had to be chosen.

III. Polarization Division Multiplex (PolDM) Transmission

PolDM means that one bit modulates the horizontal and another the vertical field. The double-one symbol can have any polarization among $\pm 45^\circ$ linear and right/left circular. An interchannel phase modulation varies the double-one polarization. Interference caused by polarization mismatch at the RX will, therefore, alternate its strength and sign. This creates an error signal for polarization control. PMD becomes detrimental if the PSPs are mixtures of horizontal and vertical. Double-ones with variable polarization alternately travel in the fast or slow PSP and suffer arrival time variations. For sinusoidal differential phase modulation, both interference signal and arrival time have Bessel spectra. Bessel lines 2, 3, and 4 are monitored to extract error signals.

The setup was modified for 2×40 Gb/s carrier-suppressed (CS) RZ PolDM transmission (Fig. 6). A second Mach–Zehnder modulator (CS-RZ), driven at 20 GHz, generated 13-ps wide

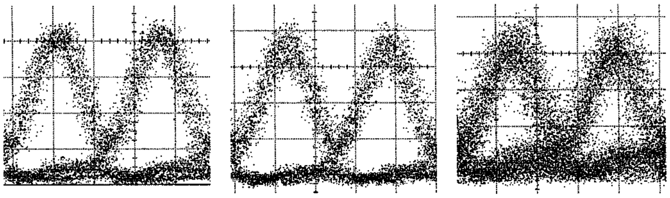

Fig. 7. Eye diagrams back-to-back (left), after 212 km with (middle) and without (right) PMDC. (Different persistences were inadvertedly taken but do not play any role).

40-GHz pulses. The data-modulated signal was split, delayed in one arm by 224 bit durations and recombined with orthogonal polarizations in a polarization beamsplitter (MUX). A frequency modulation (FM) with 240-MHz peak-to-peak width and a 417-kHz fundamental frequency was applied to the TX laser to generate interchannel phase modulation with an index $\eta = 4.2$. Total link length was 212 km (plus DCF). Powers were similar as before, but only 0 dBm was launched into the first DSF section.

In the RX, there was a single 4-ps DGD section between the polarization controllers, followed by a fiber polarizer (POL). The 40-Gb/s signal was demultiplexed to 2.5 Gb/s, where bit-error-rate (BER) was measured on one randomly chosen subchannel. Interference was measured in a separate, low-bandwidth RX and was processed digitally to control polarization. The VCO input signal was processed similarly, but with an initial integration, and served for PMD compensation. The motorized polarization transformers (M) caused endless polarization changes with ~ 0.4 rad/s speed on the Poincaré sphere, plus faster harmonic content due to discontinuous stepper motor operation. In separate measurements, each polarization channel was transmitted error free during 1 h. Nevertheless simultaneous fiber handling was possible because finite polarization changes are much easier to track than endless ones. Monitored eye diagrams back-to-back and after 212 km are shown in Fig. 7. When the link was operated only with polarization control (Fig. 7, right), but without PMDC error-free transmission was not possible.

Another laser with equal power as the first was added to investigate cross-phase modulation tolerance. Frequency separation was 400 GHz due to limited optical filter selectivity. The system was again operated error-free, but with reduced margin. Penalty was $\sim 1 \ldots 2$ dB. Finally, all fiber was taken out. The PMDC DGD was increased to 5.5 ps. Between the two motorized polarization transformers another DGD section was inserted as a PMD emulator, with a DGD of 0, 2, 4, 5.5 or 6 ps. Both for manual (seeking worst case) and motorized operations transmission was error free. Without PMDC, just with polarization control, the system was operated error-free at 2 ps, but not at $\geq$ 4 ps.

IV. Conclusion

A polarization scrambler with a single electrooptic waveplate has been employed to generate arrival time variations of a 40-Gb/s signal subject to PMD. These were estimated within 9.6 μs in the clock recovery. PMD detection sensitivity was 680 fs. A two-stage PMD compensator cleaned the received signal that was transmitted through a 19 ps PMD emulator or 210 km of fiber. PMD-compensated 2×40-Gb/s CS-RZ polarization division multiplex transmission over 212 km of fiber has also been reported. No extra optics or high-speed electronics were needed to generate error signals for PMD compensation and endless polarization control. We conclude that arrival time detection of PMD is a versatile low-cost technique with enormous sensitivity.

References

[1] N. Kikuchi and S. Sasaki, "Polarization-Mode Dispersion (PMD) Detection Sensitivity of Degree of Polarization Method for PMD Compensation," in *Proc. ECOC'99*, vol. II, Nice, France, 1999, WeA1.3, pp. 8–9.

[2] H. Sunnerud, M. Westlund, J. Li, J. Hansryd, M. Karlsson, P.-O. Hedekvist, and P. A. Andrekson, "Long-Term 160 Gb/s-TDM, RZ transmission with automatic PMD compensation and system monitoring using an optical sampling system," in *Proc. ECOC 2001*, Amsterdam, NL, Sept.-Oct. 30-4, 2001, PD.M.1.9.

[3] L.-S. Yan, Q. Yu, A. B. Sahin, Y. Wang, and A. E. Willner, "Simple bit-rate independent PMD monitoring for WDM systems," in *Proc. ECOC 2001*, Amsterdam, NL, Sept.-Oct. 30-4, 2001, TU.A.3.2.

[4] H. Rosenfeldt, C. Knothe, R. Ulrich, E. Brinkmeyer, U. Feiste, C. Schubert, J. Berger, R. Ludwig, and H. G. Weber, "Automatic PMD compensation at 40 Gbit/s and 80 Gbit/s using a 3-dimensional DOP evaluation for feedback," in *Proc. OFC*, 2001, PD27–1.

[5] R. Noé, D. Sandel, V. Mirvoda, S. Hinz, and F. Wüst, "150 fs online PMD detection within 5 μs," in *Proc. ECOC 2001*, Amsterdam, NL, Sept.-Oct. 30-4, 2001, Tu.A.3.4.

[6] R. Noé, D. Sandel, S. Hinz, M. Yoshida-Dierolf, V. Mirvoda, G. Feise, H. Herrmann, R. Ricken, W. Sohler, F. Wehrmann, C. Glingener, A. Schöpflin, A. Färbert, and G. Fischer, "Integrated optical $LiNbO_3$ distributed polarization mode dispersion equalizer in 20 Gbit/s transmission system," *Electronics Letters*, vol. 35, no. 8, pp. 652–654, 1999.

[7] A. R. Chraplyvy, A. H. Gnauck, R. W. Tkach, J. L. Zyskind, J. W. Sulhoff, A. J. Lucero, Y. Sun, R. M. Jopson, F. Forghieri, R. M. Derosier, C. Wolf, and A. R. McCormick, "1-Tb/s Transmission Experiment," *IEEE Photonics Technol. Lett.*, no. 8, pp. 1264–1266, 1996.

[8] R. Noé, S. Hinz, D. Sandel, and F. Wüst, "Crosstalk detection schemes for polarization division multiplex transmission," *IEEE J. Lightwave Techn.*, vol. 19, no. 10, pp. 1469–1475, 2001.

[9] K. Fukuchi, T. Kasamatsu, M. Morie, R. Ohhira, T. Ito, K. Sekiya, D. Ogasahara, and T. Ono, "10.92-Tb/s (273 × 40-Gb/s) triple-band/ultra-dense WDM optical-repeatered transmission experiment," in *OSA Proc. OFC 2001*, Anaheim, USA, March 17–22, 2001, PD24.

[10] S. Bigo, Y. Frignac, G. Charlet, W. Idler, S. Borne, H. Gross, R. Dischler, W. Poehlmann, P. Tran, C. Simonneau, D. Bayart, G. Veith, A. Jourdan, and J.-P. Hamaide, "10.2 Tbit/s (256 × 42.7 Gbit/s PDM/WDM) transmission over 100 km TeraLight fiber with 1.28 bit/s/Hz spectral efficiency," in *OSA Proc. OFC 2001*, Anaheim, USA, March 17–22, 2001, PD25.

[11] N. Hecker, E. Gottwald, K. Kotten, C. J. Weiske, A. Schöpflin, P. M. Krummrich, and C. Glingener, "Automated polarization control demonstrated in a 1.28 Tbit/s (16 × 2 × 40 Gbit/s) polarization multiplexed DWDM field trial," in *ECOC 2001*, Amsterdam, Netherlands, Sept.-Oct. 30-4, 2001, Mo.L.3.1.

[12] R. Noé, H. Heidrich, and D. Hoffmann, "Endless polarization control systems for coherent optics," *IEEE J. Lightwave Techn.*, vol. 6, no. 7, pp. 1199–1207, 1988.